COUPLED RANS-VOF MODELLING OF FLOATING TIDAL STREAM CONCEPTS

E. J. Ransley, **S. A. Brown** & **D. M. Greaves**, *Plymouth University, UK*
S. Hindley, *Mojo Maritime Ltd., UK*
P. Weston, *A&P Group Ltd., UK*
E. Guerrini, *Modular Tide Generators Ltd., UK*

ABSTRACT

Numerical models are now capable of providing the quantitative description required for engineering analysis. However, for structures such as floating tidal stream devices, the complex nature of the system can rarely be included using the functionality of existing models. Typically key aspects of the system are considered separately or omitted from the analysis completely, leading to uncertainties in both the power delivery and survivability of these devices. To provide a better understanding of the behaviour of such systems, a coupled Computational Fluid Dynamics (CFD) model has been developed including a floating structure, 4-point mooring system and the influence of a submerged turbine. The open-source software OpenFOAM® solves the fully nonlinear, two-phase, incompressible, Reynolds-Averaged Navier-Stokes (RANS) equations using a finite volume approach and a Volume of Fluid (VOF) method for the interface. The behaviour of the device is included via a coupled rigid-body solver, combined with a two-way actuator line representation of the turbine and a new hybrid-catenary mooring model. Full scale test cases including regular waves and currents, based on those at the Perpetuus Tidal Energy Centre (PTEC), have been investigated. The motion of the device, loads in the moorings and thrust on the turbine have been calculated and compared with those predicted by a potential flow code and mooring analysis software. It is shown that the turbine, currents and moorings have significant impacts on the structure's response, and are therefore important in assessing the fatigue life and power capture of floating tidal stream concepts.

NOMENCLATURE

A	actuator disk area (m^2)
a	turbine axial induction factor
B	constant based on roughness length
C_t	turbine thrust coefficient
d	water depth (m)
dx	perpendicular distance from turbine (m)
F_T	total thrust force on actuator disk ($kgms^{-2}$)
G	along axis Gaussian weight
H	wave height (m)
H_S	significant wave height (m)
T	wave period (s)
t	time (s)
Q	'bladed-Gaussian' weighted volume (m^3)
U_T	local fluid velocity (ms^{-1})
U_{T*}	relative local fluid velocity (ms^{-1})
U_∞	far-field fluid velocity (ms^{-1})
u	fluid velocity (ms^{-1})
$u*$	friction velocity (ms^{-1})
V_{cell}	cell volume (m^3)
z	vertical Cartesian coordinate (m)
β	'blade width' (rads)
θ_i	displacement from centre of blade i (rads)
λ	tip speed ratio
ρ	fluid density (kg/m^3)
σ	standard deviation for along axis weights

1. INTRODUCTION

Development of offshore renewable energy (ORE) industries is of high national importance to the UK. Tidal stream is predictable and the technology has a number of similarities to both hydro and wind turbines accelerating the development of concepts relative to nascent industries like wave energy [1].

The majority of established tidal stream devices, however, are still based around seabed-mounted or gravity-based structures, limiting the number of viable deployment sites due to depth and bathymetry constraints. Furthermore, currents tend to reduce with depth making these devices sub-optimal in terms of power delivery. In addition to this, established concepts have tended to include very large diameter rotors in order to increase the total power capture of the device and hence reduce the overall cost of energy. However, the size of the devices and the seabed location leads to time-consuming and difficult installation, maintenance and recovery procedures typically requiring specialist vessels and large weather windows. This ultimately reduces the availability of the device as well as the annual power capture whilst simultaneously increasing the overall costs.

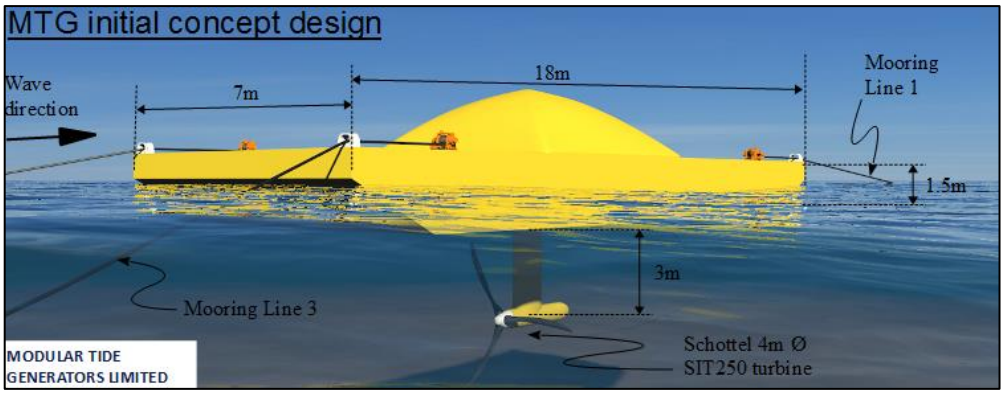

Figure 1: The Modular Tide Generators Ltd initial concept design.

In contrast, floating tidal stream concepts: can exploit more potential sites as they are not limited to shallow water or level bathymetry; can access the highest flow speeds near the surface, and; tend to be much easier to install, maintain and recover as they can simply be towed into place using non-specialist vessels and secured using a relatively simple mooring arrangement. As a result, a number of floating tidal stream concepts have been proposed and are presently in development [1]. Despite this, being located at the free-surface adds a number of additional design considerations, most notably exposure to waves and the dynamic respond of the device. This leads to concerns over both the power delivery and survivability of these devices and there is now a requirement for a better understanding of the behaviour of floating tidal stream concepts when exposed to wave excitation.

It is now common in offshore and coastal engineering to use numerical modelling to provide the quantitative description required for analysis [2]. As a result, a huge range of models have been developed to provide a better understanding of the conditions experienced by structures when subject to ocean waves and currents. However, when it comes to floating tidal stream concepts, existing numerical models rarely include the required functionality for modelling the complex system of nonlinear hydrodynamics, floating hull, mooring systems and submerged turbines. Typically, key components of the system are treated separately or omitted and models are often linearised leading to uncertainties in terms of power delivery and survivability (particularly in large waves and strong currents). In order to provide a better understanding of the behaviour, mooring loads and power output of floating tidal stream systems in realistic hydrodynamic conditions, a coupled, fully nonlinear numerical model is required.

The aim of this work is therefore, to develop an open-source, efficient and sustainable, numerical tool for assessing complete coupled floating tidal stream systems including the floating hull, mooring system and a submerged turbine in fully nonlinear wave and current conditions. Simulations have been performed at full-scale in hydrodynamic conditions based on those at the Perpetuus Tidal Energy Centre (PTEC) site and the device's motion, mooring loads and turbine output compared with existing simplified models.

2. METHODOLOGY

The method used in this work utilises the open-source software OpenFOAM® to solve the fully nonlinear, incompressible, Reynolds-Averaged Navier-Stokes (RANS) equations for air and water using the finite volume method and a Volume of Fluid (VOF) treatment of the interface [3]. The coupled behaviour of the complete device is included via a new library incorporating a series of new turbine and mooring-line models into the existing 6DOF rigid-body motion solver.

2.1 FLOATING HULL

For the purpose of this investigation, the Modular Tide Generators (MTG) initial concept design has been utilised (Figure 1). The buoyant part of the device is 18m long, 7m wide and 1.5m deep. The 'barge' is based on existing barge designs with a moon-pool in the centre to accommodate a 4m diameter turbine module. The initial concept is constructed from steel and has a mass of 60te. Ballast weighing 22te has been added and when the 1.32te turbine and 10te support structure are included the moon-pool is covered level with the hull [4].

2.2 COMPUTATIONAL MESH

The parametrically-designed domain is 420m long, 60m wide and 90m tall (33m of air, 57m of water). The background mesh is constructed using cubic cells with a side length of 2m. At the free-surface the mesh is refined two levels using the octree refinement strategy. Around the turbine and on the surface of the barge the mesh is refined up to five levels. To accommodate the motion of the device the deformable region of the mesh has been given an inner radius of 3m and an outer radius of 26m. This ensures a sufficient, but not excessive, region of deformable mesh whilst maintaining the mesh quality close to the device [3].

2.3 MOORING MODEL

The mooring system is comprised of four hybrid-catenary lines each consisting of 85m of synthetic line and 150m of chain. In this study, the nonlinear nature of each mooring line has been included using a new 'look-up table' method that calculates the three-component reaction force for each line from a matrix of values derived manually over a Cartesian grid using the dynamic analysis software OrcaFlex® [5]. Tri-linear interpolation is used at every time step to ascertain the precise reaction force for each mooring line (based on the position of the barge) and apply it to the barge's equation of motion in the form of a 'restraint' [4]. The dynamics of the mooring lines themselves and the influence of the fluid flow on the mooring force (e.g. through drag or vortex induced vibrations) have not been included, nor has the influence of the mooring line on the fluid.

2.4 TURBINE MODEL

2.4 (a) Actuator-type turbine model

Including fully blade-resolved turbine models in CFD is extremely compute-intensive prohibiting their use in routine design applications (especially for floating devices) [6]. Therefore, additional functionality has been written for OpenFOAM® to allow the presence of a submerged turbine to be included in the CFD model without the need to fully resolve the turbine's blades in the mesh.

An actuator-type method [7,8] has been used, in which the turbine properties are assumed to be wholly described by the radius of the swept area of the turbine and a thrust coefficient,

$$C_t = 4a(1-a), \tag{1}$$

where a is the axial induction factor linking the free-stream velocity, U_∞, in the axial direction to the instantaneous local velocity, U_T, by

$$\frac{U_\infty}{U_T} = 1 - a. \tag{2}$$

The total thrust force, F_T, on the disk is then

$$F_T = \tfrac{1}{2} A U_\infty^2 C_t \rho = 2 A U_{T*}^2 \rho \left(\left(\frac{1}{1-a} \right) - 1 \right), \tag{3}$$

where A is the disk area, ρ is the fluid density and U_{T*} is the difference between U_T and the turbine velocity due to the motion of the barge.

Here, a 'turbine region' made up of cells within a cylindrical region with the same radius and sharing an axis with the turbine is assumed. The local velocity, U_T, is approximated as the ratio of the vector sum of Gaussian-weighted velocities within this region to the sum of the weights,

$$G = \frac{1}{\sigma\sqrt{2\pi}} \exp\left(-\frac{dx^2}{2\sigma^2} \right), \tag{4}$$

where dx is the perpendicular distance from the turbine and σ is the Gaussian root mean squared (RMS) width [4]. The cylindrical region has a total axial length of 4σ with the turbine positioned centrally. The weights are radially uniform. The total thrust force on the turbine can then be found at runtime, using Equation 3, without any prior knowledge of the incident flow field.

To couple the thrust on the turbine with the subsequent reduction in fluid momentum, a net equal and opposite 'body force' is applied over the turbine region via an additional source-term in the momentum equations. The body force in each cell is the ratio between the total thrust force, F_T, and the cell's 'bladed-Gaussian' weighted volume

$$Q = \frac{G}{\beta\sqrt{2\pi}} \exp\left(-\frac{\theta_i^2}{\beta^2} \right) . V_{cell}, \tag{5}$$

where V_{cell} is the cell volume, β is the 'blade width' in radians, of wedge-shaped 'blades', and θ_i is the angular displacement from the centre of blade i. To give a simple approximation to the rotational nature of real turbines, the centre line position of

each blade is then up-dated at every time-step according to the angular velocity of the turbine.

This formulation allows for the influence of the moving turbines to be included easily and ensures smooth variations in both thrust and body force without a complex mesh or re-meshing at runtime. This greatly reduces the CPU effort, compared to blade-resolved models, but, although the thrust on the turbine is theoretically accurate, complex flow structures near the blades and in the wake region are not likely to be captured correctly.

2.4 (b) Turbine properties

The turbine properties have been based on the 4m diameter Schottel Hydro SIT250 turbine [9]. The rotor has 3 blades and β has been set to $\pi/8$. Above a cut-in speed of 1ms^{-1}, the turbine has a region of constant $C_t = 0.671$ and tip speed ratio, $\lambda = 4.5$. At rated power (62kW) the turbine has an over-speed control incorporating flexible blades leading to an axial induction factor and λ that depend on the incident flow speed. These, as well as the power output and r.p.s. of the turbine, have been approximated using a polynomial fit to existing turbine data [10]. The turbine has been assumed to perform identically with the flow direction reversed and with the turbine stationary, the model has been found to predict the total thrust, power and the theoretical U_T value, to within 1%.

2.5 HYDRODYNAMIC CONDITIONS

In order to place the test cases performed here in the context of realistic hydrodynamic conditions, the wave and current conditions used have been based on those recorded at the PTEC site, a proposed demonstration facility to support the development of tidal energy technologies. The site is situated in the English Channel, approximately 2.5km south of St Catherine's Point on the Isle of Wight. The average depth is ~57m [11].

2.5 (a) Observed current data

The Isle of Wight is surrounded by areas of strong tides. The approximate mean spring peak and mean neap peak surface flow rates have been estimated, from ADCP data, at between 2.5 and 2.9ms^{-1} and 1.3 and 1.6ms^{-1} respectively [11]. The tidal regime within the proposed development site is characterised by current speeds which are generally greater immediately below the water's surface than those at depth [11]. However, the measured velocity profiles do not appear to follow either a seventh- or a tenth-power law. Therefore, a fit of the von Karman-Prandtl equation,

$$u = \frac{u^*}{\kappa}\log\left(u^*(z+d)\right) + B \tag{5}$$

has been used to approximate the current profile at the site where z is the vertical dimension, d is the water depth, u^* is the friction velocity, $\kappa = 0.4$ and B is a constant based on the roughness length [12]. For neap tides, $B = -1.8$, $u^* = 0.09$ matches the measured data well. For spring tides $B = -2.24$, $u^* = 0.13$ was an improvement over power law profiles but still has some discrepancies near the seabed.

2.5 (b) Wave climate

The English Channel is open to the Atlantic Ocean in the south-west and with the dominant south-westerly weather systems the Isle of Wight is open to strong wind-wave and swell conditions. Despite this, the wave climate at the PTEC site is quite often (22.67% of the time) calm (H_S below 0.5) making the average conditions relatively low [11]. Of more interest are the hydrodynamic conditions at the limit of the device's operational window. It is under these conditions that the effect of various complexities in the system will be most obvious. Therefore, the waves selected for this study are based on a Weibull fit to the wave data from the south-west (the predominant wave direction) with a return period of 1 year. This gave a wave height, H, of 6.1m, a wave period, T, of 9s and a wave steepness of 0.15 [10]. The joint probability of spring currents (~ 1 hour every 14 days) and the 1-in-1 year significant wave height (~ 3 hours every year), coinciding for at least one minute, gives this case a return period of around 85 years (typical of the design limit state of offshore structures).

2.5 (c) Numerical wave generation and absorption

In this work, the waves and currents are generated using expression-based boundary conditions for the surface elevation and fluid velocity. The waves are prescribed using Stokes second-order theory with a 4.5s ramp-up. The current velocity profiles

are applied to both the wave-maker boundary and the opposite boundary based on Equation 5.

The initial conditions are set using the flow field solution in current-only cases after100s. This allows the barge and flow field to reach a pseudo-steady state before the waves are added using a linear superposition of the two conditions.

Wave (and current) absorption is achieved using the 'relaxation zone' formulation distributed with the additional toolbox 'waves2Foam' [13]. A 30m relaxation zone with a third-order polynomial weighting is positioned next to the wave-maker boundary to absorb waves scattered by the barge. A 2-wavelength long (240m) relaxation zone, with exponential weighting, is positioned on the opposite boundary. One wavelength should be sufficient to absorb 99% of the wave [13] however, when including both waves and currents it was found that a longer relaxation zone was required.

3. RESULTS AND DISCUSSION

Using the numerical tool described above, a series of full-scale simulations have been run with the entire MTG concept and Schottel SIT250 turbine model included. A number of combined wave and current conditions based on those at PTEC have been considered including both peak spring and

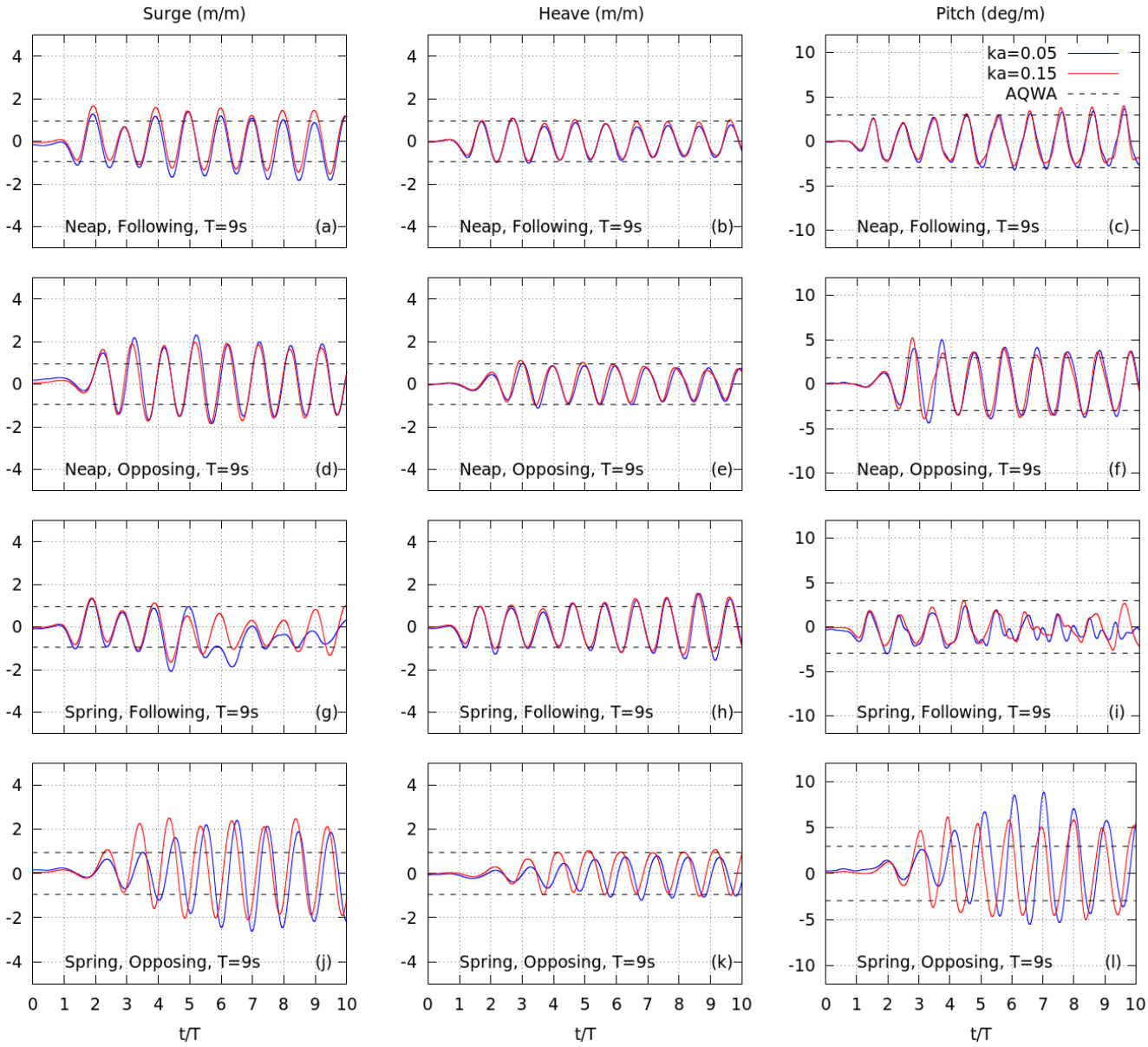

Figure 2: Surge (left), heave (centre) and pitch (right), normalised by the wave amplitude, *H/2*, for the 1-in-1 year wave (red) and a lower steepness wave (blue), in neap following (top), neap opposing (second row), spring following (third row) and spring opposing (bottom) currents based on those at the PTEC site. Also plotted are the amplitudes of motion predicted by Ansys® AQWA™ in the wave-only case (dashed).

peak neap currents in directions both following and opposing the waves. Two unidirectional regular wave conditions have been used: the 1-in-1 year wave described above (H = 6.1m, T = 9s, steepness=0.15) and a lower steepness wave (H= 2m, T=9s, steepness=0.05).

Simulations were performed using the ARCHER high performance computing facility (Cray XC30 system) on 48 cores. Each had an execution time of between 30 and 40 hours (~1680 CPU hours). In general, the less steep waves took slightly less time to complete (~48 CPU hours shorter) as did the opposing wave cases.

Figure 2 shows the normalised motion of the barge in each of the test cases. The amplitude of motion predicted by the potential flow solver AQWA^{TM} has also been plotted. AQWA^{TM} uses linear wave theory so that when normalised by the wave height it is not able to differentiate between waves of different steepness. Furthermore, the effect of the mooring system and the addition of currents cannot be easily included in AQWA^{TM} and so these have been omitted from the model. Finally, in AQWA^{TM} nonlinear effects are ignored and all degrees of freedom of the device are decoupled.

The results in Figure 2 show that, in these two cases the wave steepness has a minimal effect

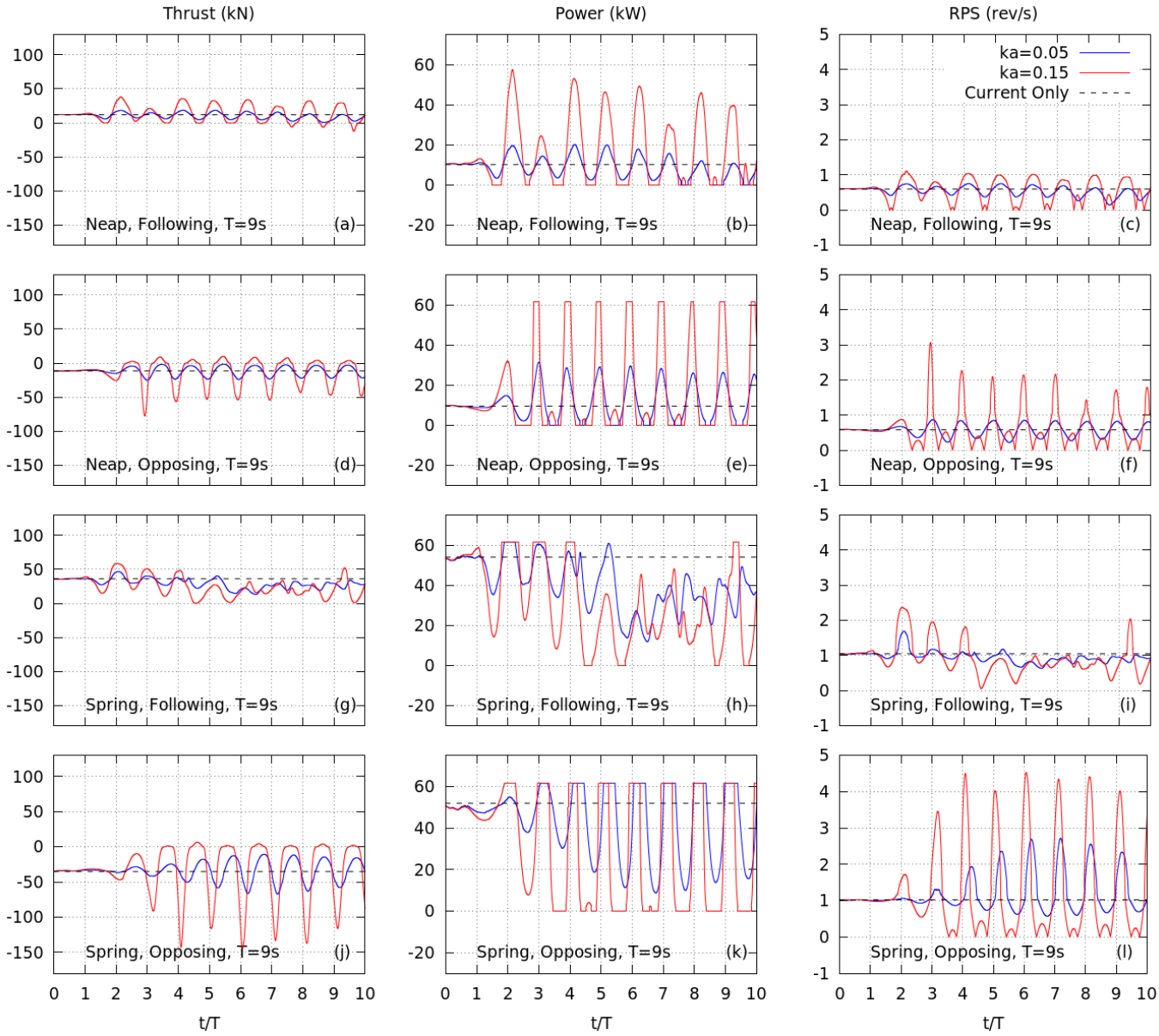

Figure 3: Thrust on the turbine (left), electrical power generated (centre) and r.p.s. of the rotor (right), for the 1-in-1 year wave (red) and a lower steepness wave (blue), in neap following (top), neap opposing (second row), spring following (third row) and spring opposing (bottom) currents based on those at the PTEC site. Also plotted are the recorded in the absence of waves *i.e.* currents only (dashed).

on the motion of the device (when normalised by the wave amplitude). The simplified AQWA™ model predicts the amplitude of motion in some cases well (particularly the heave motion), however, the amplitudes in both surge and pitch are under-estimated for opposing currents and there is some far more complex behaviour present in the spring following case. These observations are due to the combined effect of the mooring system stiffness and the modulation of the incident wave due to the presence of the currents; opposing currents tend to increase the steepness of incoming waves and, hence, one might expect higher amplitude motions. For the spring following case the high frequency behaviour observed is as a consequence of the barge being violently over-topped by the waves following a period of strong restoring force in the bow mooring lines.

Figure 3 shows the measured thrust on the turbine, the power output and the r.p.s. of the rotor for the same cases as in Figure 2. Also shown are the measured mean results in the absence of waves, *i.e.* current-only. It can be seen that, the presence of waves and the motion of the device lead to large, (mostly) periodic variations in these three parameters. This is of particular concern to turbine

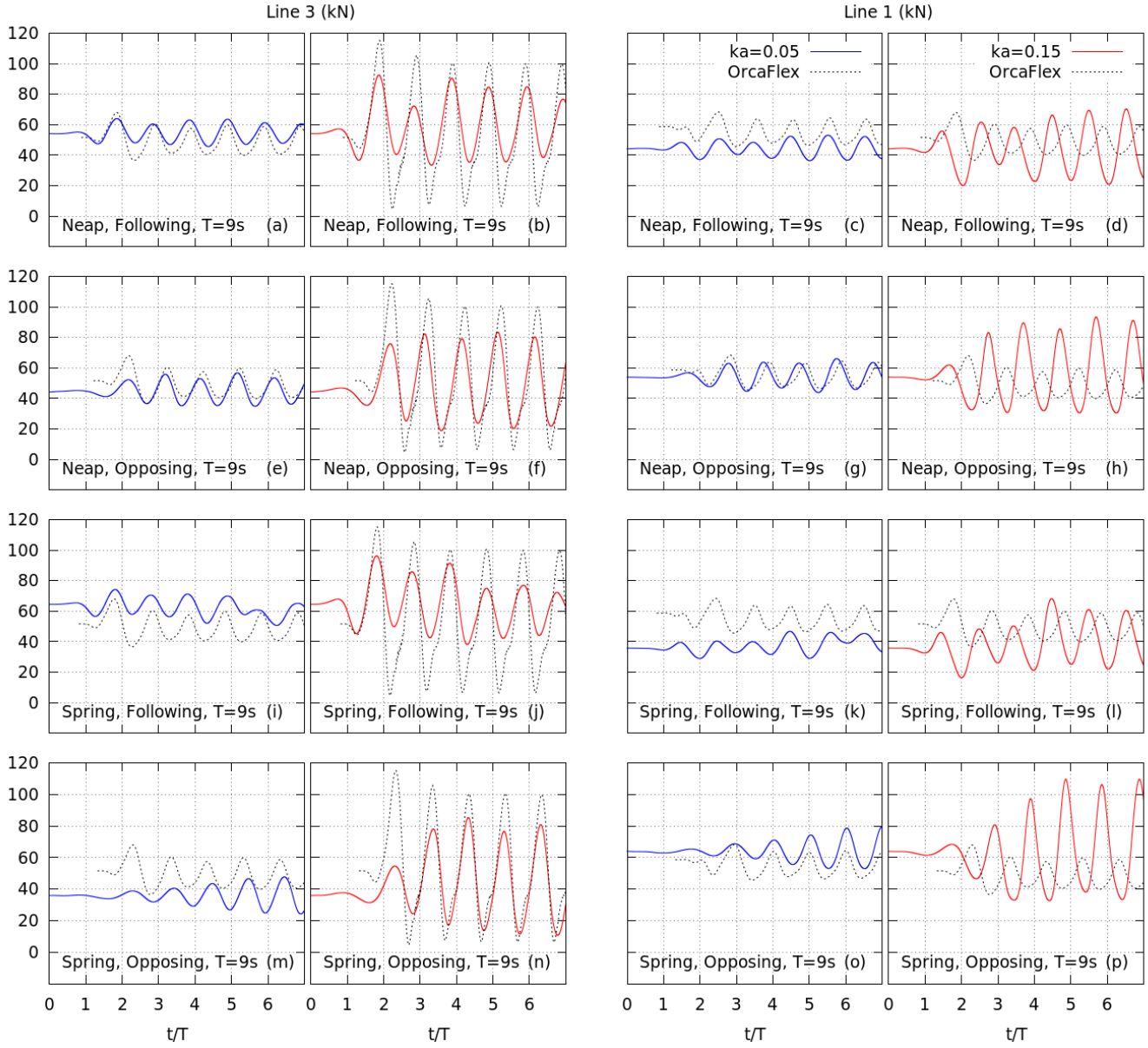

Figure 4: Tension in two of the mooring lines: Line 3 (left) on the up-wave side of the barge, Line 1 (right) on the down-wave side of the barge, for the 1-in-1 year wave (red) and a lower steepness wave (blue), in neap following (top), neap opposing (second row), spring following (third row) and spring opposing (bottom) currents based on those at the PTEC site. Also plotted are the time series of the mooring loads predicted by Orcaflex® dynamic analysis software in the wave-only case (dotted).

developers in terms of both power delivery and the fatigue life of the turbine units. It can also be seen that, due to the nonlinearity of these parameters, there are considerable differences between the results for the two wave steepnesses. The steeper (larger) of the two waves creates high amplitude variations which, in the opposing current cases give a high (negative) thrust and power saturation as the turbine reaches its maximum (rated) power as well as significant increases in r.p.s. due to the over-speed control strategy. The large variations in these cases also lead to moments of zero thrust and even reversed flow (positive thrust) resulting in periods with no power generation and high frequency changes in r.p.s. These will undoubtedly reduce the net power output, when compared to calm conditions, as well as raise concerns over the long-term reliability of the turbine.

It is evident that there exists a strong coupling between the motion of the barge and the turbine properties. This is possibly most notable in the spring following cases where the complex motion has resulted in reduced periodicity in the power output as well as arguably more constant r.p.s. Perhaps this is evidence that, 'design' of the system's response to wave excitation could aid in mitigating undesirable fluctuations in the turbine parameters or even enhance desirable effects.

Finally, Figure 4 shows the tension in two of the mooring lines for the same test cases as in the previous two figures. Line 3 and Line 1 are attached on the up-wave and down-wave side of the device respectively (see Figure 1). The tensions predicted by dynamic analysis software Orcaflex®, without currents included, have also been plotted. Orcaflex® relies on a linearised model for the motion of the barge and, once again, the various degrees of freedom are decoupled from one another. It is possible to include an approximation for the effect of the currents and the thrust on the turbine by means of a linearised drag coefficient, but this would still have to be derived using a separate model and so has been omitted from this study. In each case in Figure 4, the first peak in Line 3's load has been aligned with the Orcaflex® result and the same time shift applied to Line 1's time series.

Including the effect of the currents and the thrust of the turbine clearly effects the tension in the mooring lines. At the beginning of each of the time series, before the waves arrive, a clear shift is observed with the upstream mooring, *i.e.* Line 3 in opposing currents, having increase tension and the downstream mooring, *i.e.* Line 3 in following currents, having decrease tension (relative to that predicted by Orcaflex®, *i.e.* no currents). This is due to the offset in the barge's position caused by the current-induced thrust on the barge and turbine. Furthermore, the Orcaflex® model predicts much higher amplitude loads in Line 3, *i.e.* the line nearest the wave maker, as well as a considerable amount of nonlinearity (particularly in the steeper (larger) of the two wave cases). Conversely, Orcaflex® predicts lower amplitude loads in Line 1, *i.e.* on the down-wave side of the barge, and there is a phase shift in the steeper wave case when compared to the CFD result. The CFD model predicts comparable loads in both the aft and bow lines which may be preferable in terms of mooring system design and device survivability. These patterns do not appear to be influenced by the current direction suggesting that the coupled nature of the barge's various degrees of freedom is responsible for moderating the effect of waves on the mooring load. As well as potentially beneficial effects on the various turbine properties, this may be evidence that, 'designing' the device's response to waves could be used to mitigate against high mooring loads and allow for more cost effective moorings systems to be used.

4. CONCLUSIONS

A fully nonlinear open-source CFD approach has been presented, including a RANS-VOF solver coupled with a rigid-body solver, new model for hybrid-catenary mooring systems and a new actuator line-type model for submerged turbines.

A series of full-scale simulations have been performed in conditions based on those at the Perpetuus Tidal Energy Centre (PTEC) site just off the southern tip of the Isle of Wight, using the Modular Tide Generators (MTG) initial concept design and turbine characteristics based on the Schottel SIT250 turbine.

The motion of the device, thrust on the turbine, power generated and r.p.s. of the rotor, as well as the mooring loads, have been recorded in test cases involving the 1-in-1 year wave (H = 6.1m, T= 9s) and a less steep wave of the same frequency (H = 2m, T = 9s) combined with peak

neap and peak spring tides both following and opposing the waves.

The motion of the device in surge, heave and pitch has been compared with the amplitude of motion predicted by the potential flow code AQWA^{TM} where the simplified linear model neglects the influence of the turbine, the mooring system and the currents and treats the various degrees of freedom separately. It was found that the steepness of the wave did not affect the motion dramatically and the AQWA^{TM} model predicted the amplitude of heave motion well. However the surge and pitch motion in opposing currents was under-estimated and the potential flow code was also unable to predict complex nonlinear behaviour observed in steep waves and following current conditions.

The thrust on the turbine, power generated and r.p.s. of the rotor were all shown to experience large amplitude fluctuations and undesirable features such as power saturation, high frequency accelerations and periods of zero output when subject to waves. Furthermore, the nonlinearity of these parameters meant there were significant differences between waves of different sizes and steepnesses. In the spring following cases there is evidence of strong coupling between the turbine parameters and the motion of the device leading to speculation that control of the barge's behaviour in waves could reduce the undesirable oscillations experienced by the turbine or even enhance the power capture of floating tidal stream concepts.

The tension in two of the mooring lines has been compared with that predicted by the dynamic analysis software Orcaflex® in the absence of currents. It was shown that the currents produce a reduction in the mean tension of downstream lines and an increase in the upstream lines but that the current direction did not significantly influence the amplitude of the periodic mooring loads. The CFD model predicted comparable mooring loads in both mooring lines whereas, in the steeper wave case, Orcaflex® predicted much higher loads in the up-wave line than the down-wave line. This is again evidence that the coupled nature of the system may be responsible for, in this case, desirable impacts on various design parameters.

In conclusion, it is clear that each of the components involved in a floating tidal stream concept are strongly coupled and capable of influencing important design considerations. In order to understand the true behaviour, power delivery and survivability of such systems, before going to the expense of full-scale deployment, coupled numerical models such as the one described here are crucial.

ACKNOWLEDGEMENTS

The authors acknowledge that, this work used the ARCHER UK National Supercomputing Service (http://www.archer.ac.uk) and has been funded as part of Innovate UK Project 102217 through the Energy Catalyst Early-stage Round 3 and in connection with the Collaborative Computational Project in Wave Structure Interaction (CCP-WSI) EP/M022382/1.

REFERENCES

1. King, J., Tryfonas., T., 2009, 'Tidal stream power technology – state of the art, *in Proceedings of OCEANS 2009 – Europe, 11-14 May 2009: Bremen, Germany*.
2. BMT Fluid Mechanics Ltd., 2001, 'Review of model testing requirements for FPSO's', *Health and Safety Executive*.
3. Ransley, E., 2015, 'Survivability of Wave Energy Converter and Mooring Coupled System using CFD', *PhD thesis, Plymouth University, UK*.
4. Ransley, E., Brown, S., Greaves, D., Hindley, S., Weston, P., Guerrini, E., Starzmann, R., 2016, 'Coupled RANS-VOF Modelling of Floating Tidal Stream Concepts', *in Proceedings of the 4th Marine Energy Technology Symposium (METS), 25-27 April 2016: Washington, D.C., USA.*
5. Orcina, 2016, 'Orcaflex', online at *https://www.orcina.com/SoftwareProducts/OrcaFlex/*, accessed August 2016.
6. Masters, I., Williams, A., Croft, N., Togneri, M., Edmunds, M., Zangiabadi, E., Fairley, I., and Karunarathna, H., 2015, 'A Comparison of Numerical Modelling Techniques for Tidal Stream Turbine Analysis', *Energies, 8, pp. 7833-7853*.
7. Burton, T., Sharpe, D., Jenkins, N., Bossanyi, E., 2001, 'Wind Energy Handbook', John Wiley & Sons, Ltd..
8. Twidell, J., Gaudiosi, G. (eds), 2009, 'Offshore Wind Power', Brentwood: Multi-Science Publishing.

9. SCHOTTEL HYDRO, 2014, ‘Cost-effective power from currents’. SCHOTTEL HYDRO GmbH, Germany.
10. Ransley, E., Brown, S., Greaves, D., Hindley, S., Weston, P., Guerrini, E., Starzmann, R., 2016, ‘RANS-VOF Modelling of Floating Tidal Stream Systems’, *in Proceedings of the 5th Oxford Tidal Energy (OTE) Workshop, 21-22 March 2016: Oxford, UK.*
11. Royal HaskoningDHV, 2014, ‘Chapter 7: Physical Processes’, *in ‘Perpetuus Tidal Energy Centre (PTEC), Environmental Statement’, Royal HaskoningDHV, Amersfoort, Netherlands.*
12. Dyer, K. R., 1970, ‘Current Velocity Profiles in a Tidal Channel’, *Geophys. J. R. astr. Soc. 22, pp. 153-161.*
13. Jacobsen, N., Fuhrman, D., and Fredsøe, J., 2012, ‘A wave generation toolbox for open-source CFD library: OpenFOAM®’, *Int. J. Numer. Meth. Fluids, 70, pp. 1073-1088.*